Silica Nanotube Reactors for Catalytic Polymerization of Styrene and Olefins

Joong Jin Han,[1] *Sang Yool Lee,*[1] *Sang Bok Lee,*[2] *Kyu Yong Choi**[1]

Summary: Silica nanotube reactor (SNTR) has been designed and used as a novel catalytic polymerization reactor device to synthesize syndiotactic polystyrene (sPS), and polyethylene with $Cp^*Ti(OCH_3)_3$ and *rac*-Et(indenyl)$_2ZrCl_2$ metallocene catalysts in conjunction with methylaluminoxane (MAO). The highly crystalline sPS molecules polymerized within the SNTR form nano-scale polymeric fibrils of 30–50 nm in diameter that further intertwine to fill the nanopore. The polymer molecular weight of sPS has been found to increase significantly in the SNTR. A simplified mathematical reaction model for the SNTR suggests that hindered chain transfer reactions in the nanopores filled with rigid polymeric nanofibrils might have caused the extended polymer chain length. The morphological characteristics of polymeric nanofibrils and the effect of SNTR's geometric confinement on the polymer properties are also discussed. It is also demonstrated that the liberated SNTR can be a novel 'See-Through' tool for visual observation when it is analyzed by transmission electron microscopy.

Keywords: mathematical modeling; metallocene catalysts; polyethylene; polyethylene; silica nanotube reactors; syndiotactic polystyrene

Introduction

Silica nanotube reactor (SNTR) is a novel catalytic reactor system that consists of an array of straight and cyclindrical pores/channels of 20-200 nm in diameter where active catalyts compounds are covalently deposited onto a silica surface.[1] Unlike in mesoporous silica fibers (MSF) or mesoporous silica such as MCM-41 that has pores in the range of 2–50 nm-diameter, the pores in the SNTR can be made large (~200 nm-diameter) to allow for the diffusion of bulky molecules such as styrene monomer from a bulk fluid phase into the pores where active catalytic sites are present. Anodized alumimum oxide (AAO) films are used as a basic frame for a silica nanotube reactor. AAO film is formed by the electrochemical oxidation of aluminum with a hexagonal arrangement of monodisperse nanopores. In recent years, AAO films are widely used as templates for the synthesis of a wide variety of functional nanostructures.[2–5]

The present work has been motivated from our previous study of syndiotactic styrene polymerization with homogeneous and heterogeneous metallocene catalysts ($Cp^*Ti(OCH_3)_3$/MAO) where nanofibrillar polymer morphologies were observed.[6–8] Although the fragmentation of silica occurs with a buildup of polymer in a silica-supported metallocene catalyst system, the polymers grow as long nanofibrils of about 30–50 nm-diameter.[8] The nanofibrillar particle morphology of syndiotactic polystyrene (sPS) is very unique and significantly different from the globular morphology that is commonly observed in polyolefins (e.g., polyethylene, polypropylene) synthesized over heterogeneous catalysts such as Ziegler-Natta catalysts

[1] Department of Chemical and Biomolecular Engineering, University of Maryland, College Park, MD 20742, U.S.A.
E-mail: choi@umd.edu
[2] Department of Chemistry and Biochemistry, University of Maryland, College Park, MD 20742, U.S.A.

or silica-supported metallocene catalysts. The origin of fibrillar growth of sPS or its growth mechanism over heterogenized metallocene catalysts during the polymerization is not fully understood. The rapid crystallization of sPS with δ-form crystalline structure in a hydrocarbon liquid (i.e., mixture of styrene and diluent) is believed to drive the formation of 2_1-helix that may promote the surface interaction of the polymer chains to form intertwined nanofibrils. It has been also reported that sPS-solvent compounds (or intercalates) in many hydrocarbon solvents have the 2_1 helical structure.[9–11] In this paper, we discuss the polymer morphology development in a silica nanotube reactor as well as some interesting effects on the polymer properties.

Experimental Part

Materials

We used two different types of metallocene catalysts: pentamethyl cyclopentadienyltitanium trimethoxide ($Cp^*Ti(OCH_3)_3$ (Strem Chemicals)/MAO (Albemarle, 10% in toluene, 4.55 wt% Al content)) for styrene polymerization, and *rac*-$Et(indenyl)_2ZrCl_2$ (Boulder Scientific)/MAO for ethylene polymerization. Styrene was chosen as a bulky monomer and ethylene was chosen as a non-bulky monomer. Styrene (Aldrich) was vacuum distilled over calcium hydride, and inhibitor was removed by activated alumina. *n*-Heptane (Fisher Scientific) was used as a solvent and purified by being refluxed over sodium and benzophenone under a nitrogen atmosphere. Polymerization grade ethylene was purified by passing through a purification column packed with molecular sieves (Type 4A, Grace Davison), Cu catalyst (R3-11, BASF), and neutral alumina (Aldrich). Toluene was purified using activated molecular sieves.

Silica Nanotube Reactor (SNTR)

An anodized aluminum oxide (AAO) porous film was used to fabricate a nanotube reactor. Two different AAO films (200 nm pores (Whatman) and 60 nm pores) were used in our experiments. The 60 nm AAO films were synthesized in our laboratory using the methods described elsewhere.[12,13] It is noted that both pore ends are open in 200 nm-diameter AAO films whereas only one pore end is open in 60 nm-diameter AAO films. Table 1 lists the basic properties of the AAO films used in our study.

The pore surfaces of the AAO films were coated with silica by the surface sol-gel method.[1] An AAO film was first soaked in $SiCl_4$ solution, quickly immersed and washed with fresh hexane 4 times to remove unabsorbed $SiCl_4$. The AAO film was placed in methanol/hexane (1:1 v/v) mixture and then ethanol before drying in nitrogen flow. The film was immersed in a deionized water, washed with methanol and dried. This procedure was repeated several times to obtain a 3–7 nm thick layer of silica at the pore surface. Before supporting metallocene catalyst onto the inner pore walls of an SNTR, the SNTR film was treated twice with MAO solution in toluene at ambient temperature for 24 h, washed with toluene, and dried in vacuo. To deposit the catalyst, the SNTR film was mixed with a catalyst solution in toluene at ambient temperature for 24 h, washed with toluene,

Table 1.
Basic properties of anodized aluminum oxide (AAO) films.

AAO film properties	AAO Film 1 (Whatman)	AAO Film 2 (U of Maryland)
Pore diameter	200 nm	60 nm
Film thickness	60 μm	5 μm
Pore density	10^9 pores/cm^2	2.1×10^{10} pores/cm^2
Pore surface area	3.77×10^{-7} cm^2/pore	9.42×10^{-9} cm^2/pore
Average surface area	2.3 m^2/g	23 m^2/g
Pore volume	1.88×10^{-12} cm^3	8.48×10^{-14} cm^3

and dried in vacuo. To remove the metallocene catalyst exposed to the bulk liquid phase, the top and bottom surfaces of the SNTR film were mechanically polished. This procedure ensures that the polymerization occurs only in the nanopores in the SNTRs.

Polymerization

In styrene polymerization, the catalyst-deposited SNTR film was placed in a 20 mL glass bottle containing a liquid mixture of styrene and *n*-heptane. The reaction bottle was placed in a constant temperature chamber at 70 °C. After polymerization, the reaction bottle was emptied and the reaction mixture was washed with an excess amount of methanol and then dried in vacuo. For the polymerization of ethylene, we used an 100 mL glass reactor (pressure rating: 50 psig) and the partial pressure of ethylene was kept constant during the polymerization.[14]

Polymer Analysis

Scanning electron microscopy (SEM) analysis of dried SNTR/polymer samples were carried out using Hitachi S-4700 SEM. The samples were coated with AuPd layer in a Denton DV-503 vacuum evaporator. Transmission electron microscopic (TEM) analysis was carried out using Zeiss EM10CA and differential scanning calorimetry (DSC) analysis was performed at a heating rate of 20 °C/min under nitrogen atmosphere using Q1000 (TA Instruments). Syndiotacticity of sPS was measured by ^{13}C NMR spectroscopy using a Bruker 500 Mhz DRX-500 spectrometer. The polymer solution was prepared by dissolving in 1,1,2,3-tetrachloroethane-d_2 (~1 mg/mL). To characterize the molecular weights of sPS samples, a high temperature gel permeation chromatograph (PL GPC 220, Polymer Laboratories) was used with trichlorobenzene (TCB) as a solvent at 160 °C. The crystalline structure of the polymer samples were investigated by X-ray diffraction (XRD) analysis using Bruker D8 Advanced with GADDS (Bruker AXS).

Results

Syndiotactic Polystyrene

Morphology

As the SNTR film was placed in a reaction bottle, the top surface of the film became cloudy as the polymer formed inside the nanopores moved out of the pores. Figure 1 shows a photograph of the SNTR film during the polymerization and the white mass of sPS accumulating above the SNTR. The polymer mass resembled a 'cotton candy'. After the polymerization, the entire mass of the polymer and the SNTR film were removed from the reaction bottle and dried. It was confirmed that the white mass above the SNTR film was bound to the top surface of the film. As the sample was dried, the white mass of the polymer above the SNTR film collapsed onto the top of the SNTR surface.

Figure 2 shows the SEM images of a typical polymer morphology of sPS synthesized in the SNTR of 200 nm-diameter pores. Here, a part of the polymer layer above the flat SNTR film surface was removed to reveal the SNTR top surface. The SNTR film was also fractured to observe the side of the film. In Figure 2(a), we can observe that the top polymer layer consists of sPS nanofibrils of about 30–50 nm in diameter. The dimension of the nanofibrils observed in Figure 2(a) is very similar to that observed in the slurry polymerization of styrene over silica-supported $Cp^*Ti(OCH_3)_3$/MAO catalyst.[8]

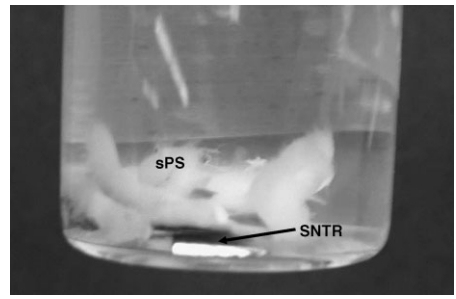

Figure 1.
Syndiotactic polystyrene extruded out from the nanopores of an SNTR film (70 °C).

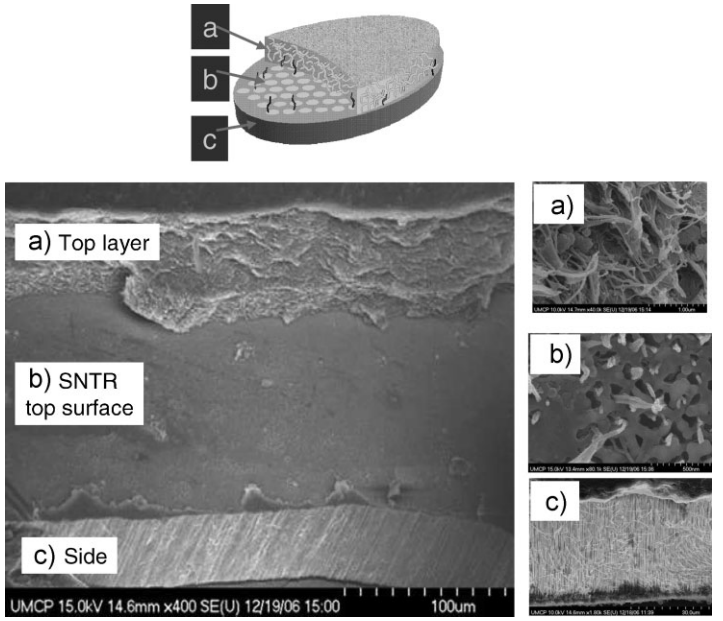

Figure 2.
SEM images of sPS nanostructures: (a) vertical cross-section of the polymer layer on the SNTR film surface, (b) top-down view of the surface of the polymer layer, (c) vertical cross-section of the polymer-filled nanopores.

Figure 2(b) shows the sPS nanofibrils extruding out from the pores as intertwined nanofibril bundles. It is a clear evidence that polymerization occurred inside the silica coated nanopores of the SNTR. It is interesting to observe that some pores are fully filled with polymeric nanofibrils but some other pores are only partially filled with polymer nanofibrils. Some pores are empty but it is believed that the polymers in these pores were pulled out as the top polymer layer was removed during the sample preparation. Indeed, the side view of the fractured SNTR film (Figure 2(c)) shows that the pores (or nanochannels) were filled with sPS nanofibrils. From the X-ray diffraction analysis, it was found that the sPS nanofibrils have a δ-form crystalline structure.

Syndiotacticity

The syndiotacticity of sPS synthesized in SNTRs was measured by ^{13}C NMR spectroscopy. Surprisingly, it was found that the syndiotacticity of the sPS nanofibrils was 100% (i.e., single peak at 44.3 ppm in the 43.0–47.0 ppm range). With the same $Cp^*Ti(OCH_3)_3$/MAO catalyst used in either homogeneous or silica-supported catalyst system, the syndiotacticity was about 93–96%.[6–8,15] Therefore, our experimental result suggests that the syndiospecificity of the active catalytic sites may be affected by the presence of sPS nanofibrils that fully occupy the nanopores of the SNTR. At this point, we are not able to offer a plausible mechanism of polymer chain propagation leading to 100% syndiotacticity. This will be an interesting problem to investigate in the future work.

Dimension of sPS Nanofibrils

We also carried out an experiment with the metallocene catalyst deposited onto a flat surface to investigate whether the geometric confinement imposed by the nanopores may cause the formation of sPS nanofibrils. Here, the question is whether the basic dimension of the sPS nanofibrils (30–50 nm) observed in the SNTR can be regarded as a characteristic dimension of sPS nanofibrils. To this purpose, we carried

out a polymerization experiment using a flat catalyst surface where no spatial confinement effect is present. As a catalytic reaction platform, we used a silicon wafer: One side of a silicon wafer surface was first oxidized to amorphous silica, and the wafer was soaked in piranha solution for surface treatment. The surface-treated wafer that now has surface hydroxyl groups was washed with excess amount of acetone. Before depositing the catalyst onto the wafer surface, the wafer was treated with MAO solution at 50 °C for 24 hr, washed with toluene, and dried in vacuo overnight. Then the MAO treated silicon wafer was immersed in $Cp^*Ti(OCH_3)_3$ solution, washed with toluene, and finally dried in vacuo overnight. The polymerization of styrene was carried out using a glass tube reactor at 70 °C for 12 hr. Figure 3 illustrates an SEM image of the wafer surface.

It is interesting to observe that indeed the sPS nanofibrils growing from the flat catalytic surface are of about 30–50 nm in diameter, which is consistent with the size of nanofibrils observed in the SNTRs. Therefore, it appears that the size of primary sPS nanofibrils from the heterogeneous catalytic polymerization is 30–50 nm.

Molecular Weight Distributions (MWDs)

Another interesting and important observation from this work is that the molecular weight of sPS synthesized over SNTRs was significantly higher than the sPS synthesized over either homogeneous or silica-supported catalyst. Figure 4 shows the comparison of molecular weight distribution curves of sPS synthesized in SNTRs ($M_w = 928{,}000$), a slurry reactor with silica-supported catalyst ($M_w = 221{,}000$), and a slurry reactor with homogeneous catalyst ($M_w = 198{,}000$). The silica-supported catalyst and homogeneous catalyst show similar molecular weight characteristics probably because the disintegration of silica-sPS particles may result in a minimal geometric confinement effect on the growth and/chain transfer of the sPS chains. The nanochannels in the SNTRs do not disintegrate during the polymerization and as shown earlier, sPS extrudes out as intertwined 'nano-ropes' that almost completely filled the pore space. It suggests that during the entire initiation-growth-chain transfer period, the sPS chains may experience severe geometric confinement effect imposed by the mass of 'nano-ropes' in the pores. As a result, the chain transfer rate decreases and the polymer chain length increases. Figure 4 also shows that in the MWD curve for the SNTR polymer, about 40 wt.% of sPS has a molecular weight larger than 1,000,000 g/mol, with the largest molecular weight detected by gel permeation chromatography as large as 5 million g/mol. The extremely large molecular weight as observed in the SNTR system has never been reported in the literature on sPS with heterogeneously supported metallocene catalysts.

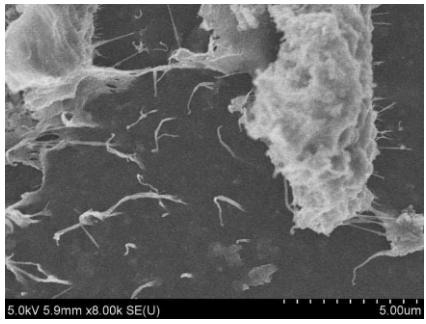

Figure 3.
Nanofibrils of sPS on a flat catalyst surface.

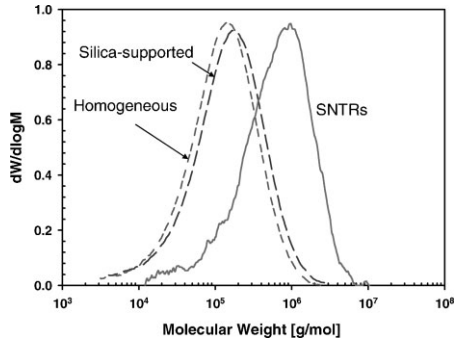

Figure 4.
Molecular weight distributions of sPS: SNTRs (200 nm; $M_w = 928{,}000$), Silica supported catalyst ($M_w = 221{,}000$), Homogeneous catalyst ($M_w = 198{,}000$).

Kinetic Modeling

To develop a quantitative understanding of the polymerization kinetics for styrene polymerization to sPS in a SNTR system, we consider the following kinetic model.

Catalyst site activation:

$$C_0 + MAO \xrightarrow{k_a} C^* \quad (1)$$

Chain propagation:

$$\begin{aligned} C^* + M &\xrightarrow{k_p} P_1 \\ P_n + M &\xrightarrow{k_p} P_{n+1} \end{aligned} \quad (2)$$

Chain transfer to monomer:

$$P_n + M \xrightarrow{k_{tM}} M_n + P_1 \quad (3)$$

β-hydrogen elimination:

$$P_n \xrightarrow{k_{t\beta}} M_n + C^* \quad (4)$$

Catalyst deactivation:

$$\begin{aligned} C^* &\xrightarrow{k_d} D^* \\ P_n &\xrightarrow{k_d} M_n + D^* \end{aligned} \quad (5)$$

where C_0 is the potent catalyst site, C^* is the activated catalyst site, P_n and M_n are the live and dead polymer chains of length n, M is the monomer, and D^* is the deactivated catalyst site. k_j represents the reaction rate constant for each corresponding reaction. The polymerization rate equations and molecular weight moment equations for this model can be found elsewhere.[4] Based on the above kinetic scheme, Han et al.[16] developed a two-site model for styrene polymerization over silica-supported $Cp^*Ti(OCH_3)_3$/MAO catalyst and the model parameters were optimized to fit the experimentally observed MWDs. It was assumed that the MWD follows the composite of the Schulz-Flory distribution function for each site type: $W_i(x) = \tau_i^2 x \exp(-\tau_i x)$ where x is the chain length and $W_i(x)$ is the weight chain length distribution for the polymer produced by site i. The model parameter is defined as $\tau_i = (k_{tM}[M]_s + k_{t\beta} + k_d)/k_p[M]_s$. The overall weight chain length distribution is calculated by the following equation: $W_{tot}(x) = \sum_{i=1}^{N} \phi_i x W_i(x)$ where ϕ_i is the weight fraction of the site type i (The details of the model equations can be found elsewhere[16]). Their simulation results for the silica-supported $Cp^*Ti(OCH_3)_3$/MAO catalyst system agreed very well with the experimental data. Thus, we applied the same two-site model to the styrene polymerization in the SNTR, but the molecular weight distribution predicted by the model deviated significantly from the experimental data as shown in Figure 5(a).

For addition polymers such as sPS, either chain propagation rate should be very large and/or chain transfer rate should be very small to obtain high molecular

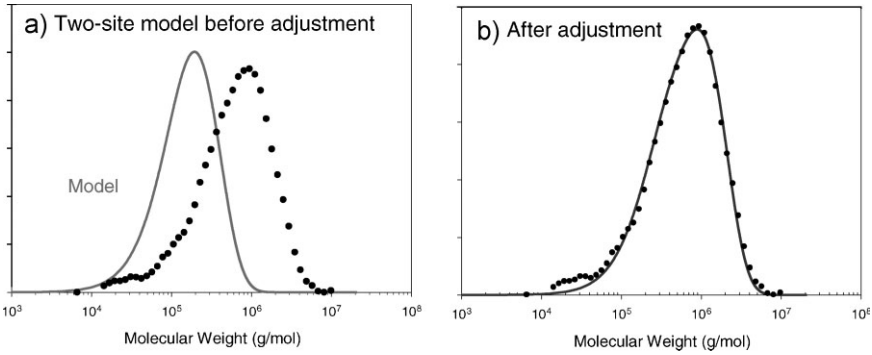

Figure 5.
sPS molecular weight distributions (symbols-data, lines-model simulations): (a) MWD predictions with a two-site kinetic model for silica-supported $Cp^*Ti(OCH_3)_3$/MAO catalyst, (b) MWD predictions with pore-length dependent β-hydride transfer rate constant.

weight. Certainly, it is unlikely that the polymerization rate (i.e., chain propagation rate) in the nanopores will be higher than in the silica-supported catalyst system because the monomer concentration in the presence of polymer nanofibrils filling the nanopores is expected to be low because of diffusion resistance. Indeed, as we calculated the monomer concentration with pore diffusion limitations, the polymerization rate was found to be low and the monomer diffusion had no effect on the increase in the molecular weight.

If there is no significantly enhanced chain propagation reaction rate in the SNTR, the only possible cause for higher molecular weight might be related to chain transfer reaction rates. According to the sPS polymerization literature, it is generally agreed that β-hydride elimination is the primary mode of chain transfer reaction.[15] For the purpose of fitting the experimentally observed molecular weight distribution data with the kinetic model, we use the following empirical equation to vary the β-hydride chain transfer rate constant along the pore length: $k_{t\beta} = k^0_{t\beta} e^{-(i-1)}$. Here, $k^0_{t\beta}$ is the chain transfer rate constant used for the silica-supported catalyst and the index i represents the position index in the pores as the entire pore is divided to a finite number of zones. In other words, in this empirical model, we are assuming that the β-hydride chain transfer rate constant decreases exponentially from the pore entrance because the deep interior of the SNTR filled with the polymer may provide less favorable chain transfer reaction environment than near the pore entrance. With this empirical factor incorporated into the kinetic model, the MWD curve was recalculated for the SNTR system and the calculated MWD was very well matched by the model simulation results (lines, Figure 5(b)). Although there is little theoretical evidence for such position-dependent chain transfer rate constant as used in our calculations, the results shown in Figure 5 indirectly suggest that more analysis would be necessary to understand the polymer growth and chain transfer mechanisms in the SNTRs.

Transmission Electron Microscopy (TEM) Image

We also observed the sPS nanofibrils inside the 60 nm SNTR by transmission electron microscopy. The silica nanotubes containing sPS were liberated after dissolving alumina selectively in a 0.1 M NaOH solution. Figure 6 illustrates the TEM images of the nanotubes containing sPS nanofibrils. Note that most of the nanotubes are not fully filled with sPS, probably because the pores were not large enough for these secondary sPS nanofibrils (c.a. 30 nm) to intertwine to larger size. It is interesting to observe that the sizes of the sPS nanofibrils are nearly constant along the nanotube length, suggesting that the polymerization occurred uniformly throughout the interior of SNTR pores. Figure 6 also indicates that the SNTR is an interesting and novel tool to observe the growth of polymers in catalytically active pores or channels. In other words, the SNTR can be used as a ''See-Through Window'' for the polymer growth in heterogeneously catalyzed polymerization systems.

Ethylene Polymerization in SNTRs

We also carried out ethylene polymerization experiments at 70 °C using a silica nanotube reactor and Figure 7 illustrates an SEM image of the SNTR after polymerization. It shows that SNTR can be successfully used to polymerize ethylene. The overall morphological characteristics of the polymer in the nanopores are similar to those of sPS but it is quite apparent that polyethylene nanofibrils are much softer

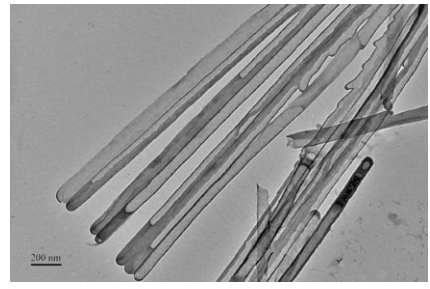

Figure 6.
TEM image of sPS in SNTRs (60 nm-OD).

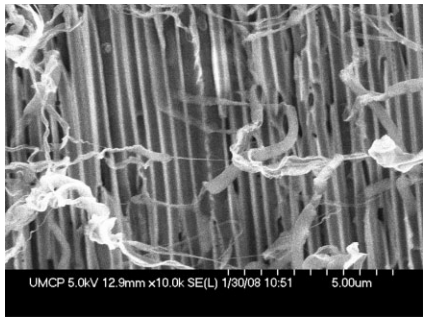

Figure 7.
Cross-sectional view of a silica nanotube reactor in ethylene polymerization at 70 °C.

than sPS and it is easily seen that some of the intertwined nanofibrils form thin 'tape-like' structures. Although we have not measured the polymerization rate or catalytic activity in the SNTR, it is expected that the overall catalytic behavior is very similar to that of a silica-supported catalyst because of similarity of the surface characteristics.

Concluding Remarks

In this paper, we have presented the experimental study of styrene and ethylene polymerizations with metallocene catalysts in novel silica nanotube reactor (SNTR) systems derived from anodized aluminum oxide films. The rapidly crystallizing sPS in styrene-*n*-heptane phase is characterized by the formation of δ-form crystal and the multi-stage intertwining of polymer nanofibrils inside the nanopores before moving out of the pores. The sPS synthesized with SNTRs shows higher syndiotacticity and significantly higher molecular weight than those synthesized over either homogeneous or silica-supported catalyst systems. Although we are not able to provide a conclusive interpretation of how the physical effects such as pore filling and geometrical confinement affect the polymerization kinetics and MWD of sPS, the preliminary model analysis suggests that the β-hydride chain transfer reaction may be significantly reduced in the SNTR. The SNTR was also used for ethylene polymerization and it was observed that the nanofibrillar growth of polyethylene was similar to that of sPS. However, softer polyethylene nanofibrils seemed to intertwine to form tape-like structures instead of rigid nanofibrils observed in sPS polymerization. The SNTR can also be used as a See-Through Window device because the SNTR containing polymers inside can be easily liberated and observed by transmission electron microscopy. More detailed study of the morphological development and reaction kinetics of the polymerization for these reaction systems are in progress.

[1] K. Y. Choi, J. J. Han, B. He, S. B. Lee, *J. Am. Chem. Soc.* **2008**, *130*, 3920.
[2] D. T. Mitchell, S. B. Lee, L. Trofin, N. Li, T. K. Navanen, H. Söderlund, C. R. Martin, *J. Am. Chem. Soc.* **2002**, *124*, 11864.
[3] C. C. Harrell, S. B. Lee, C. R. Martin, *Anal. Chem.* **2003**, *75*, 6871.
[4] S. J. Son, J. Reichel, B. He, M. Schuchman, S. B. Lee, *J. Am. Chem. Soc.* **2005**, *127*, 7316.
[5] W. Lee, R. Ji, U. Gösele, K. Nielsch, *Nature Materials* **2006**, *5*, 741.
[6] J. S. Chung, B. G. Woo, K. Y. Choi, *Macromol. Symp.* **2004**, *206*, 375.
[7] H. W. Lee, J. S. Chung, K. Y. Choi, *Polymer* **2005**, *6*, 5032.
[8] J. J. Han, W. J. Yoon, H. W. Lee, K. Y. Choi, *Polymer* **2008**, *49*, 4141.
[9] B. Ray, S. Elhasri, A. Thierry, P. Marie, J. M. Guenet, *Macromolecules* **2002**, *35*, 9730.
[10] O. Tarallo, V. Petraccone, V. Venditto, G. Guerra, *Polymer* **2006**, *47*, 2402.
[11] C. Daniel, *Macromol. Symp.* **2007**, *251*, 1.
[12] S. J. Son, J. Reichel, B. He, M. Schuhman, S. B. Lee, *J. Am. Chem. Soc.* **2005**, *127*, 7316.
[13] S. J. Son, S. B. Lee, *J. Am. Chem. Soc.* **2006**, *128*, 15974.
[14] S. Y. Park, K. Y. Choi, K. H. Song, B. G. Jeong, *Macromolecules* **2004**, *36*, 4216.
[15] N. Tomotsu, N. Ishihara, T. H. Newman, M. T. Malanga, *J. Mol. Catal. A: Chem.* **1998**, *128*, 167.
[16] J. J. Han, W. J. Yoon, H. W. Lee, K. Y. Choi, *Polymer* **2007**, *48*, 6519.

